Graphical Abstract

Numerical and experimental investigation of piezoelectric energy harvester based on flag-flutter

Marco Eugeni, Hassan Elahi*, Federico Fune, Luca Lampani, Franco Mastroddi, Giovanni Paolo Romano, Paolo Gaudenzi

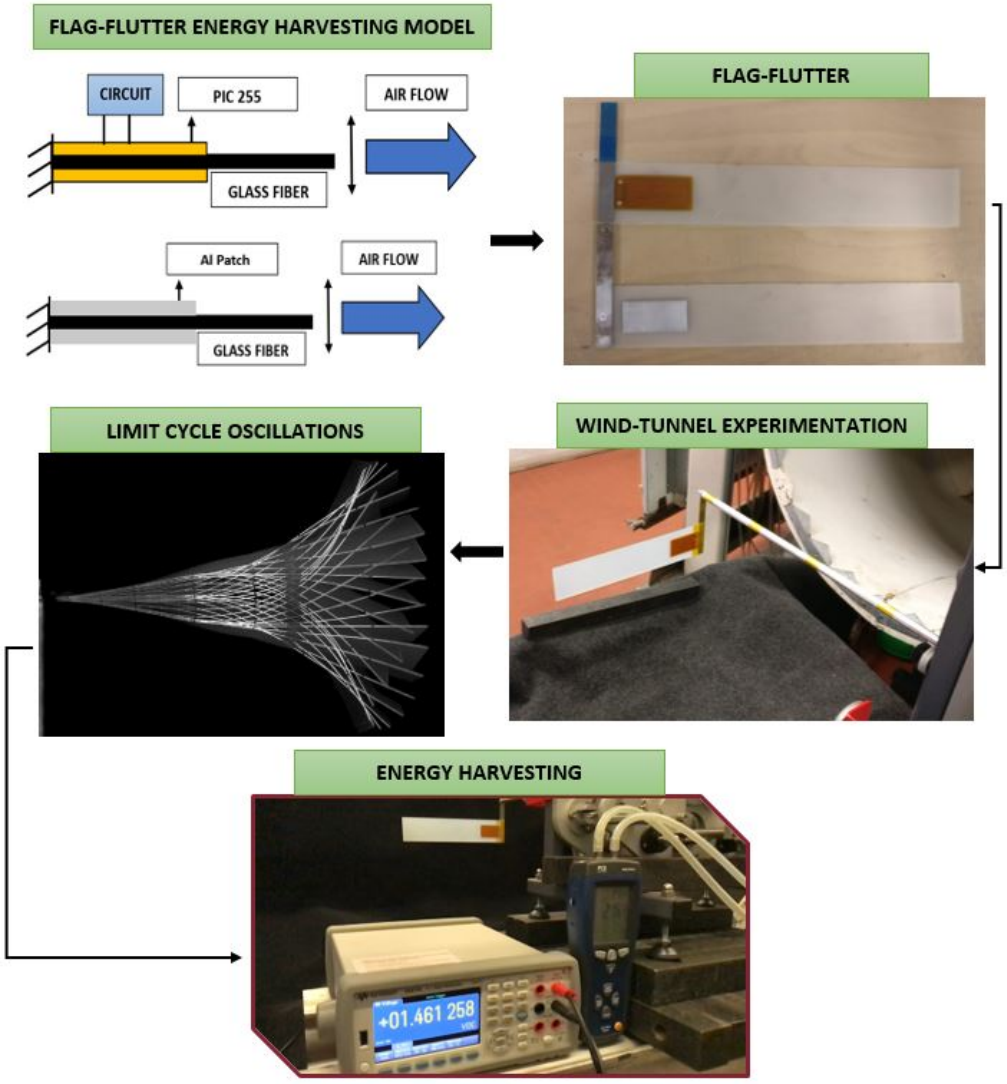

Numerical and experimental investigation of piezoelectric energy harvester based on flag-flutter

Marco Eugeni, Hassan Elahi*, Federico Fune, Luca Lampani, Franco Mastroddi, Giovanni Paolo Romano, Paolo Gaudenzi

Department of Mechanical and Aerospace Engineering, Sapienza University of Rome, Italy.
Corresponding author: hassan.elahi@uniroma1.it

Abstract

In the present era, the demand for self-powered electronic instruments is increasing and their energy consumption is decreasing. The ability to extract energy from the operating environment is of great importance in advanced industrial applications particularly in the field of aerospace. In this research, a flag-flutter based piezoelectric (PZT) energy harvester is modeled based on fluid-structure interaction (FSI) that represents an important area of research for the development of innovative energy harvesting solution. The possibility to harvest energy from Limit Cycle Oscillations (LCOs) by means of piezoelectric transduction is investigated via numerical and experimental tests. Moreover, the flutter instability of a cantilevered flag with piezoelectric (PZT) and Aluminium (Al) patches, subjected to an axial flow has been investigated. The numerical simulations are performed in MSC Nastran software and the experimental campaign is performed in a subsonic wind-tunnel. The practical interest of this instability mechanism, which can lead to self-sustained oscillations, is the possible application in flow energy harvesting. Furthermore, the critical velocities for different length of flags

are also predicted numerically and experimentally. The numerical results are in good agreement with experiments, as well as with results in the literature. The maximum power output obtained by the designed harvester experimentally is found to be 1.12 mW for 66.6 $k\Omega$ resistance. The presented model is suitable to harvest energy and to drive wireless sensors.

Keywords: Piezoelectric, Energy Harvesting, Flag-Flutter, Aeroelastic, Fluid-Structure Interaction, Subsonic Wind-Tunnel

1. INTRODUCTION

Piezoelectric materials play an important role in the field of energy harvesting as they can generate electrical energy from external stresses and this energy can be utilized to power wireless sensors or actuators having numerous applications in the field of the aerospace industry. Piezoelectric materials have high performance and can be manufactured in any scale with fewer complications [1, 2]. This energy can also be stored in batteries to perform various tasks latterly. For electromechanical interaction, two types of piezoelectricity phenomena can occur [3]. Both direct and converse piezoelectric effects have been applied since then in numerous applications, to enhance the sensorial and actuation capabilities, along with the evolution of piezoelectric materials [4]. The importance of piezoelectric based system modeling is widely emphasized in the literature, and many commercially available tools have been developed for the beam, plate and shell-type of harvesters [5, 6]. They have a wide range of applications in smart structures [7, 8] and micro/Nano-electromechanical systems [9, 10]. A lot of research has been done on the coupling of piezoelectric material for the application of energy harvesting and

many designs have been studied [11, 12]. Kim et al. investigated the detailed improved model for absorbing the vibrations from surroundings and circuitry for energy harvesting applications by combining two harvesters into one [13]. Improved circuitry can result in higher efficiency of the harvesting system and it can be improved by using variable external resistance in the circuit to predict the optimal resistance [14, 15].

The topic of energy harvesting is of significant importance from the last few decades and the development in this field has improved the micro-electromechanical systems. The piezoelectric sensors and transducers absorbing ambient energy from vibrations are very much in demand because of their energy harvesting capability [16]. The energy generated by the piezoelectric harvesters can be utilized either to power microelectronic systems, or can be stored in batteries. Many researchers have emphasized on self-powered sensors and actuators rather than relying on batteries. As batteries are heavy in weight and their maintenance cost is high; sometimes impossible i.e., in suborbital missions. So, this gap opens a chance for piezoelectric harvesters to develop self-powered portable electronic devices. The piezoelectric based harvesters are light in weight and are capable of self-dependent actuation. These harvesters are capable of operating wireless sensors i.e., for suborbital missions and have numerous applications as smart structures in the field of aerospace [17, 18, 19].

Whenever, there is an interaction between a fluid flow and a structure it is important to analyze the dynamics of the overall system built by the flow and as well as by the structure i.e., the so-called aeroelastic system [20, 21]. Mathematically, this coupling between the structure and flow happens be-

cause the natural boundary conditions (of the structure) are mutually influenced by the flow and structure. This results in an intrinsically un-stationary phenomenon, which is complex, and it is not possible to consider the flow and structure separately [22, 23]. The aeroelastic harvester tends to flap when the critical velocity of the flow arises, i.e., flutter velocity. This flutter velocity is dependent on the mechanical properties of the surrounded system and the flowing media. The aeroelastic harvester is considered not to be stable anymore in its unperturbed condition after this critical velocity of the flow and the stable oscillations arise i.e., LCOs, which tends to stabilize the system [23]. In physical terms, it means that the aeroelastic system is going through the Hopf bifurcation [24, 25]. Many researchers have worked on the self-excited oscillations as these are very rich from the dynamic point of view [24, 26]. These oscillations can play a vital role in the mechanism of energy harvesting as these oscillations can be transferred to the piezoelectric patch from the airfoil experiencing airflow. The piezoelectric patch utilizes these oscillations to harvest electrical energy [27, 28]. In designing of piezoelectric aeroelastic energy harvester (PAEH), it is important to consider the phenomenon of flutter [29]. Figure 1 depicts the sub-critical Hopf bifurcation, that occurs when the flow velocity is less than linear flutter velocity. The knee in the bifurcation diagram represents the unstable LCOs that tends into a stable one [30].

The use of piezoelectric transducers as energy harvesters by means of FSI is of great interest for aerospace applications. Many theoretical and experimental studies in a dynamic aerodynamic profile were conducted by many researchers. Woolston et al. [32] and Shen et al. [33] investigated

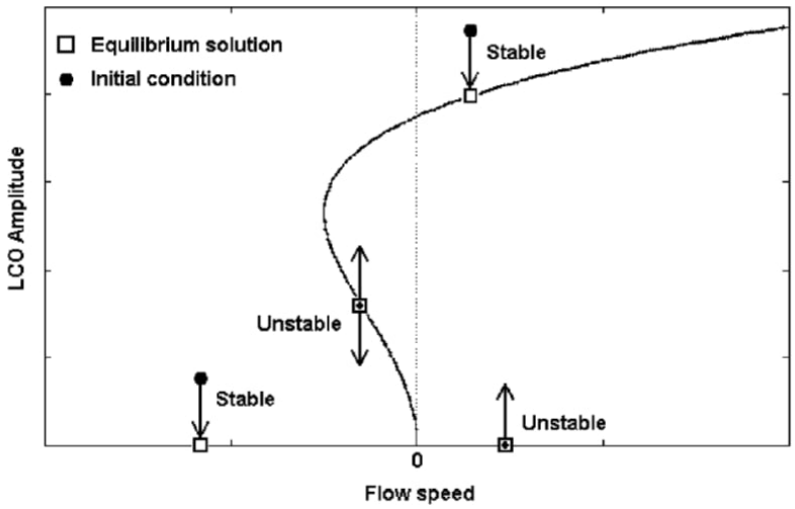

Figure 1: Sub-critical Hopf bifurcation of knee-like shape [31].

the effects of structural nonlinearity on aeroelastic systems. Yang et al. studied the effect of a freeplay nonlinearity of the typical aeroelastic system [34]. Later on, this response is analyzed experimentally and numerically by Tang et al. [35] and Conner at al. [36]. Followed by Tang and Dowell, who analyzed the freeplay nonlinearity of different aeroelastic models [37] such as, wing-store model [38], a wing section with control surface [39] and horizontal-tail model [40]. Investigations performed by them elobrates the importance of system parameters, nonlinearity and initial conditions as they affect the nonlinear aeroelastic system significantly. Elahi et al. demonstrated the importance of the aerodynamic model for the true prediction of performance and evaluation of the PAEH. Moreover, it is stressed that the evaluation of the true system stability margin is possible only if the unsteady aerodynamic model is considered [41]. Comparison of various flutter based PZT harvesters

in literature is represented in Tab. 1.

Table 1: Comparison of various flutter based PAEHs [2].

Design	Material used	Layer(s)	Power (mW)
NACA0014	PZT	1	0.003
Symmetric	PSI-5A4E	1	0.2
NACA 0012	QP 10N	2	2.2

With the perspective of using the flutter phenomenon for energy harvesting purposes, deeper comprehension of the dynamics of the fluid-structure interaction of a cantilevered flag is required. This paper aim towards the numerical and experimental evaluation of a piezoelectric energy harvester based on flag-flutter. The LCOs are the cause of energy harvesting in the designed harvester. Further, it is shown that the designed harvester is effective and can be utilized in many aerospace industrial applications to drive microelectronic devices. The energy harvesting mechanism for the flag and the numerical model of the harvester is elaborated in Section 2. The experimental campaign is discussed in Section 3. Moreover, discussion on the performance of harvester is analyzed in Section 4 and it is shown that the overall system is suitable for energy harvesting and can be utilized to drive microelectronics i.e., wireless sensors in sub-orbital missions, launchers, space vehicles and in various aerospace applications.

2. NUMERICAL MODEL

In this research work, the harvester is built by an airfoil approximated as a plate as shown in Fig. 2. The bi-morph configuration is selected for

designed harvester. Two patches of PIC 255 are attached to the glass fiber plate on the fixed end attached with external circuitry as shown in Fig. 2(a). In order to validate the model, two Aluminium (Al) patches are attached at the fixed end as shown in Fig. 2(b). When a flag is subjected to airflow, the oscillations will be transferred from a flag to the PZT patch, which results in phenomenon of energy harvesting. The overall mechanism is shown in Fig. 2. Geometric parameters of flags are represented in Tab. 2 for numerical model. The material properties of the glass fiber and the piezoelectric patch are shown in Tab. 3.

Table 2: Geometric parameters of flag (cm).

Material	**Length**	**Width**	**Thickness**
Fiber glass	15:3:38	6	0.05
Aluminium patch	5	3	0.01
Piezoelectric patch	6.1	3.5	0.01

Table 3: Material properties of glass fiber and PIC 255 [42].

Properties (unit)	**Symbol**	**Glass fiber**	**PIC 255**
Young's Modulus (GPa)	$E_1 = E_2$	21.49	62.1
	E_3	10	48.3
Shear Modulus (GPa)	G_{12}	4	23.5
	$G_{23} = G_{31}$	4	21
Poisson Coefficient	ν_{12}	0.2	0.32
	$\nu_{23} = \nu_{31}$	0.2	0.44
Density (kg/m^3)	ρ	1900	7800

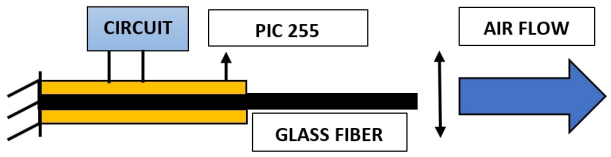

(a) Harvesting model for PZT patched flag.

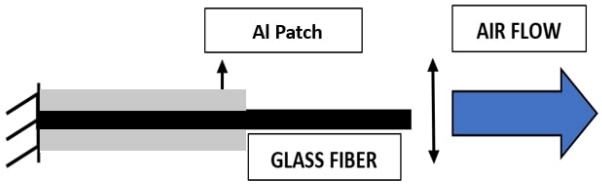

(b) Harvesting model for Al patched flag.

Figure 2: Overall harvesting mechanism.

The modeling is carried out in MSC Nastran software, which allows realizing all the laminated material components. Flags of various lengths with different configurations are modeled as represented in Fig. 3. Three different types of models are studied in numerical modeling i.e., flag with no patch attached, flag with PZT patch attached and flag with Al patch attached in order to maximize the output power, this choice allowing to explore a wide range of velocity for the flutter analysis. For aeroelastic analyses in this context, the Doublet Lattice Method (DLM) is used, which is the extension of steady vortex-lattice method to unsteady flow. For this type of analysis the solver couples flow and structure, calculating for each value of the velocity interval. The unknown lifting pressures are assumed to be concentrated uniformly across the one-quarter chord line of each aerodynamic panel. The number of nodes and elements used in meshing during the numerical analysis are

represented in Tab. 4.

Table 4: Nodes and elements for discretization.

Part	**Nodes**	**Elements**
Aluminium patch	273	240
PIC 255	273	240
Kapton layers	261	180
PZT patch	465	420
Flag (Total)	1765 (17 cm) to 2625 (38 cm)	1344 (17 cm) to 2496 (38 cm)

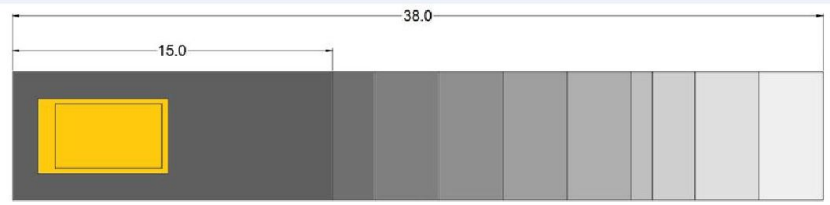

Figure 3: Geometry of the flag-flutter.

In order to predict the optimal length of the flag for energy harvesting, it is observed that due to the working mode of the PZT patch, the curvature is proportional to the voltage generated [2]. Therefore, curvature for all flags are analyzed numerically as represented in Fig. 4. From Fig. 4, it is evident that a 29 cm flag guarantees almost the same curvature, and consequently the same voltage, with less torsion than 32 cm one. Therefore, 29 cm is selected for energy harvesting in the experimental phase.

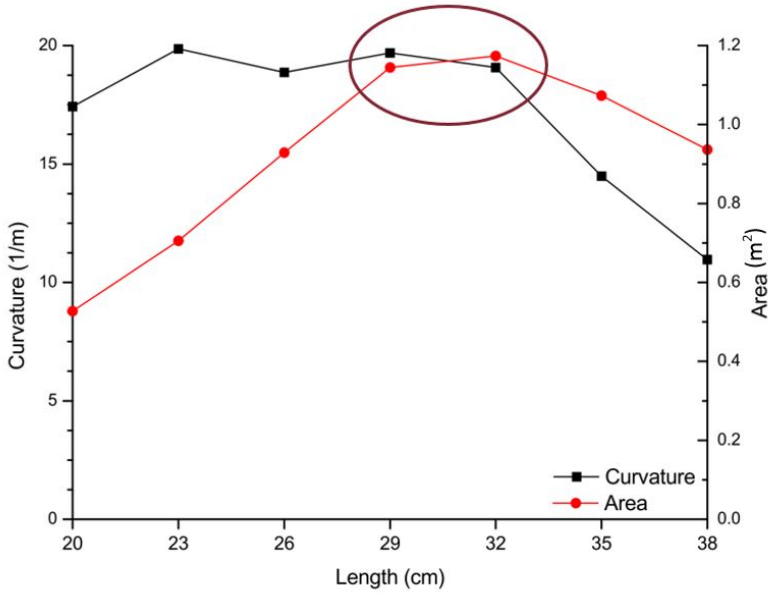

Figure 4: Normalised curvature in patch area.

3. EXPERIMENTAL SETUP

The experiments have been carried out in the structural-dynamic laboratory and wind-tunnel laboratory of the Department of Mechanical and Aerospace Engineering (DIMA), University of Rome "La Sapienza". The subsonic wind tunnel used for the experiments has a circular test cross-section with a diameter of $0.9m$ and it can provide a maximum airflow of $40m/s$.

The mean flow velocity was measured and controlled by a Pitot-static tube. A high-speed video camera, Photron Fastcam Mini AX, aligned with the vertical axis was fixed at the top of the wind tunnel. The camera was operating at $5400fps$ with a 1024×736 pixel resolution. The camera visualizations were used to extract the flutter amplitude, A, and its frequency,

f, by detecting in each snapshot of the plate the deflection of its tip. Once the test sample and camera were setup in the wind tunnel, the flow velocity was gradually increased starting from zero. At small velocities the plate appeared stable, hence steady and aligned with the flow. The critical flow velocity, U_F, is defined as the one for which the plate started flapping, whereas for $U_\infty < U_F$ every small disturbance was damped out. Once the critical flutter velocity was reached, the high-speed camera and recording of data from accelerometers were turned on and the flutter of the sample was captured for 0.175 s (i.e., 945 frames). The images were then transferred to the computer. The videos were processed later using Image Processing techniques to determine the flapping frequency and amplitude. Different configurations of flags were tried experimentally in order to investigate the aeroelastic behavior, keeping the same design. Two different configurations of flags are tested experimentally in wind-tunnel (testing system), the dimensions of the flag with the PZT and Al patch are represented in Tab. 5.

Table 5: Dimensions of flag and piezoelectric element (cm).

	Length	Width	Thickness
Flag with PZT patch	29	6	0.05
Flag with Al patch	15:3:38	6	0.05

4. Results and discussion

In order to analyze the performance of the energy harvesting mechanism for the flag-flutter, the output power was experimentally measured at variable

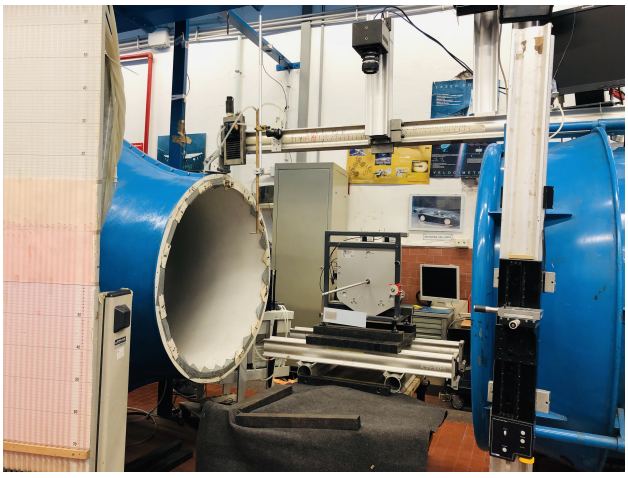

(a) Experimental setup.

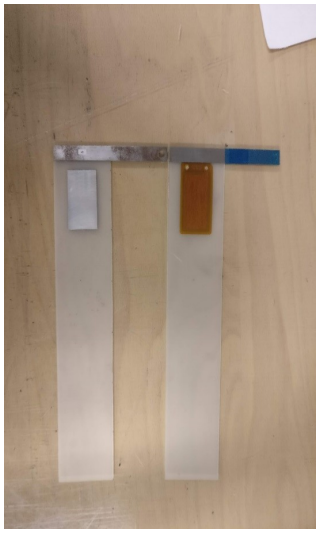

(b) PZT and Al patched flags.

Figure 5: Overall experimental campaign.

external resistance to predict the optimal one as shown in Fig. 6. The airflow was increased from zero to the critical value where the flag started flapping, these oscillations were transferred to the piezo patch from the flag resulting in energy harvesting. This harvested energy is measured in terms of power (W) by monitoring the peak to peak voltage and root mean square value via digital cathode ray oscilloscope (CRO). The output power is calculated from 0 to 1 $M\Omega$ resistances, and it was observed that the maximum peak power output obtained is 0.011 W for 66.6 $k\Omega$ resistance and after this point the output power has a negative linear behavior until 300 $k\Omega$, after this point the effect is almost constant. The possible cause for power drop at 55 $k\Omega$ is the phase misalignment between power generation by aeroelastic interaction and power absorption by the circuit.

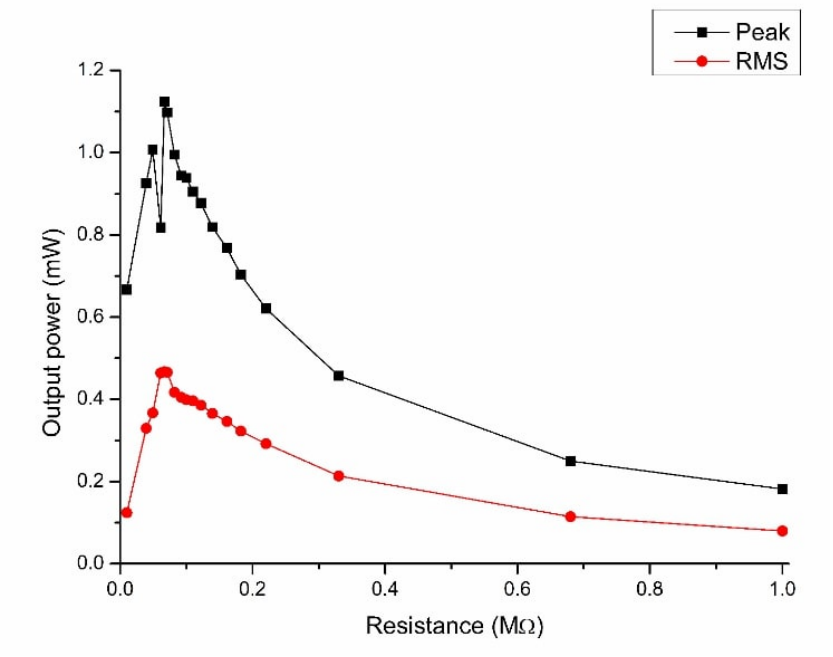

Figure 6: Optimal resistance prediction for max. output power.

To validate the numerical results with experimental ones, the flutter velocity is predicted for the different configurations of flag numerically and experimentally as represented in Fig. 7. The numerical and experimental results are in good agreement. It is observed that with increasing flag length, the critical velocity decreases.

In general, it has been observed that flutter takes place in an abrupt manner: once the flow velocity reaches a critical point, vibration develops suddenly with a large amplitude. On the other hand, when the plate is already in vibration and the flow velocity is gradually reduced, the plate may return to rest at another critical point, lower than the former one, resulting in a hysteresis loop. This hysteresis phenomenon also implies that the dynam-

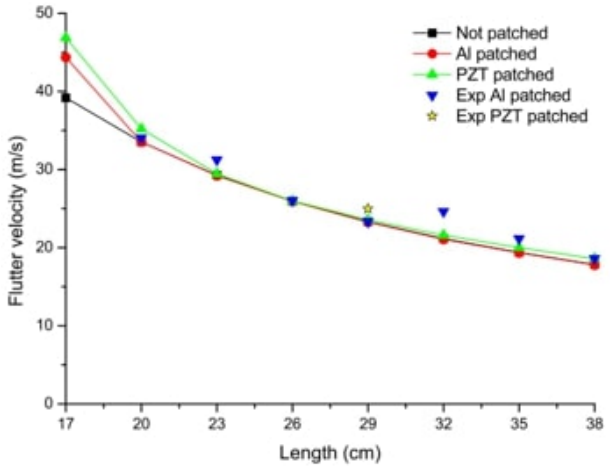

Figure 7: Numerical and experimental analysis of flag-flutter

ics depend on initial conditions; two stable states coexist between the lower and the upper critical points. Therefore, by considering the system behavior for different flow velocities, a hysteresis phenomenon has been observed for the designed flag. Different configurations were tried experimentally in order to investigate the aeroelastic behavior, keeping the same design but varying the circuit connections i.e., with open circuit (see Fig. 8), optimal resistance (see Fig. 9) and with Al patch attached (see Fig. 10). These two different configurations highlighted the effect of piezoelectric on the structural dynamics of the flag. In order to observe this trend, the flag is introduced to axial airflow by increasing gradually the flow velocity and waiting that flag flutter spontaneously, the flutter velocity occurred for a value equal to 25 m/s for PZT patched flags, while for Al patched flags it was observed to be at 23 m/s. Then, decreasing slowly the flow velocity up to 22 m/s the flag returned to its zero state for both the cases for PZT patched flags, while for

Al patched flags it was observed to be at 21 m/s. The trend of the obtained hysteresis represents a sub-critical bifurcation of fifth-order fitting for the Al patched flag. The jump is observed in both cases of optimal resistance circuit and open circuit PZT patched flags; it is proposed that this jump is due to presence of unstable branch or a due to effect of PZT patch on the flag.

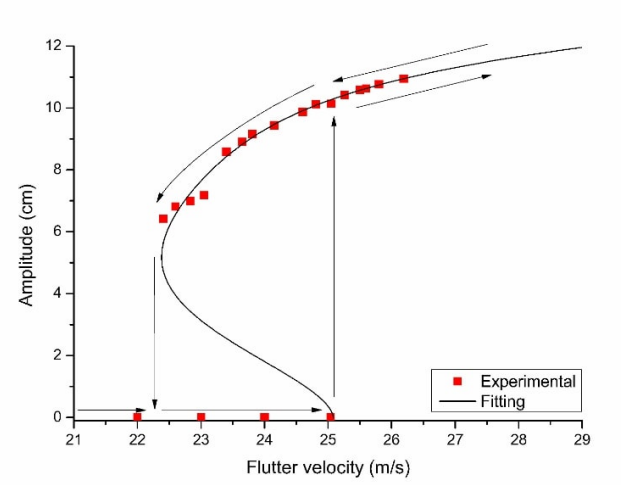

Figure 8: Bifurcation diagram for open circuit PZT patched flag.

In order to have an overview of the flutter boundary conditions, a validation of the experimental data with the literature is carried out. The same experimentation has been done by using aluminum patches instead of piezoelectric patches. The comparison of the current study with the literature [43] is represented in Fig. 11; where, the flutter boundary in terms of the mass ratio μ is shown. The present experimental data is found to be in good agreement with the theories carried out in literature [43]. The additional mass parameter in the graph can be defined as $\mu = \rho_F L/\rho_S t$ and by using $U_R/\mu = \left[(\rho_P h)^{3/2} / \left(\rho_F D^{1/2}\right)\right] U$ as an ordinate, it is possible to have a clear

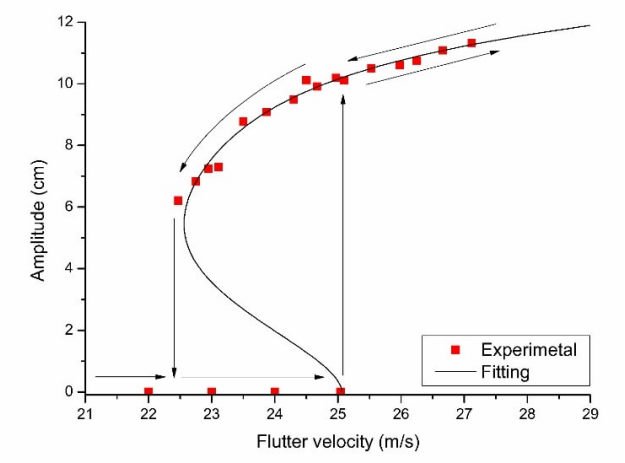

Figure 9: Bifurcation diagram for optimal resistance PZT patched flag.

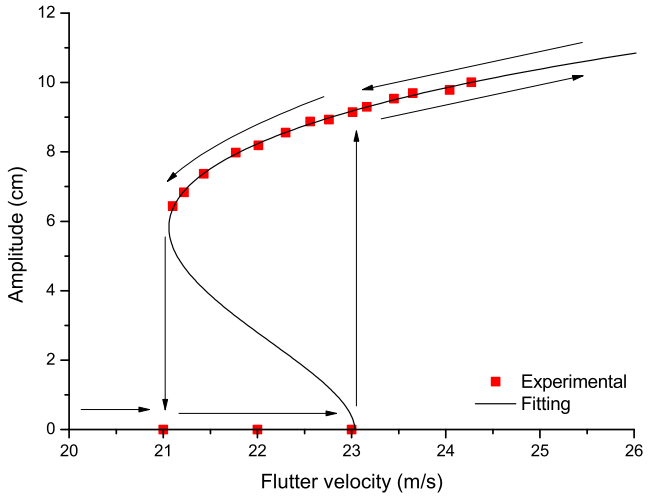

Figure 10: Bifurcation diagram for Al patched flag.

idea of flutter boundaries. Fig. 11 represents the relation between the most controllable parameters in experimentation i.e., the length of flag L, U_{RC} is

the reduced critical velocity and the critical flow velocity is U_C. It can be observed that for the small values of L, U_C is highly sensitive while it remains almost constant for the large values of L.

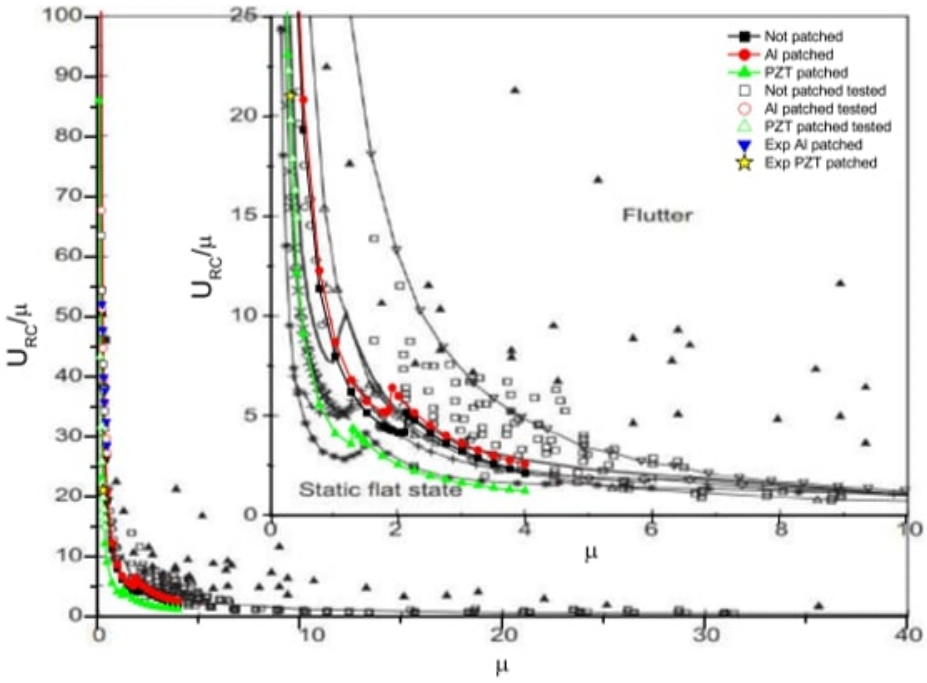

Figure 11: Comparison and validation of the numerical analysis and experimental measurements for different flags with literature (see Ref. [43]).

CONCLUSIONS

The main objective of this research is to analyze the energy harvested by the cantilevered flag and flutter instability of the flag subjected to the axial flow inside the wind tunnel. The maximum power output obtained by the designed flag is found to be 1.12 mW at optimal resistance of 66.6 $k\Omega$. The presented model is suitable to harvest energy for aerospace applications

i.e., suborbital missions and to drive wireless sensors. From the bifurcations graphs, it is found that the flutter velocity for the designed flag is 25 m/s for both the cases i.e., open circuit case and optimal resistance case and is 23 m/s for Al patched flag. The trend of the obtained hysteresis represents a knee shaped sub-critical bifurcation of fifth order fitting. A flutter boundary is obtained in the form of critical flow velocity versus the length of the flexible plate. It is found that the critical flow velocity is very sensitive to plate length when the plate is short, while it is almost invariant when the plate is sufficiently long. The flutter boundary and flutter frequencies/modes obtained using the present numerical analysis and experimentation are compared and validated with the results of other theories in the literature and it is found to be in good agreement.

References

[1] Paolo Gaudenzi. *Smart structures: physical behaviour, mathematical modelling and applications*. John Wiley & Sons, 2009.

[2] Hassan Elahi, Marco Eugeni, and Paolo Gaudenzi. A review on mechanisms for piezoelectric-based energy harvesters. *Energies*, 11(7):1850, 2018.

[3] Ahmad Safari and E. Koray Akdogan. *Piezoelectric and acoustic materials for transducer applications*. Springer Science & Business Media, 2008.

[4] Hassan Elahi, Zubair Butt, Marco Eugnei, Paolo Gaudenzi, and Asif Israr. Effects of variable resistance on smart structures of cubic recon-

naissance satellites in various thermal and frequency shocking conditions. *Journal of Mechanical Science and Technology*, 31(9):4151–4157, 2017.

[5] Hassan Elahi, Marco Eugeni, Paolo Gaudenzi, Madiha Gul, and Raees Fida Swati. Piezoelectric thermo electromechanical energy harvester for reconnaissance satellite structure. *Microsystem Technologies*, pages 1–8, 2018.

[6] Paolo Gaudenzi and Klaus-Jurgen Bathe. An iterative finite element procedure for the analysis of piezoelectric continua. *Journal of Intelligent Material Systems and Structures*, 6(2):266–273, 1995.

[7] Hassan Elahi, Marco Eugeni, and Paolo Gaudenzi. Electromechanical degradation of piezoelectric patches. In Holm Altenbach, Erasmo Carrera, and Gennady Kulikov, editors, *Analysis and Modelling of Advanced Structures and Smart Systems*, pages 35–44. Springer Singapore, Singapore, 2018.

[8] R. F. Swati, Hassan Elahi, L. H. Wen, A. A. Khan, S. Shad, and M. Rizwan Mughal. Wireless structural sensing, in: Advancedar properties of carbon fiber reinforced composites with and without piezoelectric patches for micro-crack propagation using extended finite element method. *Microsystem Technologies*, Sep 2018.

[9] Paolo Gaudenzi and Gianluca Facchini. Wireless structural sensing. In *SMART13: Smart Materials and Structures*, volume 745 of *Advanced Materials Research*, pages 155–165. Trans Tech Publications, 10 2013.

[10] K. A. Cook-Chennault, N. Thambi, and A. M. Sastry. Powering mems portable devicesa review of non-regenerative and regenerative power supply systems with special emphasis on piezoelectric energy harvesting systems. *Smart Materials and Structures*, 17(4), 2008.

[11] Dinh Gia Ninh and Nguyen Duc Tien. Investigation for electro-thermo-mechanical vibration of nanocomposite cylindrical shells with an internal fluid flow. *Aerospace Science and Technology*, 2019.

[12] Dinh Gia Ninh and Dao Huy Bich. Characteristics of nonlinear vibration of nanocomposite cylindrical shells with piezoelectric actuators under thermo-mechanical loads. *Aerospace Science and Technology*, 77:595–609, 2018.

[13] Alper Erturk, W.G.R. Vieira, C. De Marqui Jr., and D.J. Inman. On the energy harvesting potential of piezoaeroelastic systems. *Applied Physics Letters*, 96(18), 2010.

[14] G. K. Ottman, H. F. Hofmann, A. C. Bhatt, and G. A. Lesieutre. Adaptive piezoelectric energy harvesting circuit for wireless remote power supply. *IEEE Transactions on Power Electronics*, 17(5):669–676, Sep 2002.

[15] Hassan Elahi, Marco Eugeni, Paolo Gaudenzi, Faisal Qayyum, Raees Fida Swati, and Hayat Muhammad Khan. Response of piezoelectric materials on thermomechanical shocking and electrical shocking for aerospace applications. *Microsystem Technologies*, pages 1–8, 2018.

[16] L. Lampani, R. Grillo, and P. Gaudenzi. Finite element models of piezoelectric actuation for active flow control. *Acta Astronautica*, 71, 2012.

[17] Victor Giurgiutiu. Embedded nde with piezoelectric wafer active sensors in aerospace applications. *Echoes*, 1:R2, 2003.

[18] H Elahi, A Israr, RF Swati, HM Khan, and A Tamoor. Stability of piezoelectric material for suspension applications. In *2017 Fifth International Conference on Aerospace Science & Engineering (ICASE)*, pages 1–5. IEEE, 2017.

[19] Shun-Qi Zhang, Guo-Zhong Zhao, Mekala Narasimha Rao, Rüdiger Schmidt, and Ying-Jie Yu. A review on modeling techniques of piezoelectric integrated plates and shells. *Journal of Intelligent Material Systems and Structures*, 30(8):1133–1147, 2019.

[20] Maryam Hamlehdar, Alibakhsh Kasaeian, and Mohammad Reza Safaei. Energy harvesting from fluid flow using piezoelectrics: A critical review. *Renewable Energy*, 2019.

[21] Junlei Wang, Shengxi Zhou, Zhien Zhang, and Daniil Yurchenko. High-performance piezoelectric wind energy harvester with y-shaped attachments. *Energy conversion and management*, 181:645–652, 2019.

[22] Earl Dowell. *A Modern Course in Aeroelasticity*. Springer International Publishing, 2015.

[23] Earl H. Dowell and Marat Ilgamov. *Chaotic Oscillations in Mechanical Systems*, pages 285–326. Springer New York, New York, NY, 1988.

[24] John Guckenheimer and Philip J Holmes. *Nonlinear oscillations, dynamical systems, and bifurcations of vector fields*, volume 42. Springer Science & Business Media, 2013.

[25] Kai Yang, Zhen Zhang, Yanmin Zhang, and Hao Huang. High-resolution monitoring of aerospace structure using the bifurcation of a bistable nonlinear circuit with tunable potential-well depth. *Aerospace Science and Technology*, 87:98–109, 2019.

[26] Marco Eugeni, Franco Mastroddi, and Earl H Dowell. Normal form analysis of a forced aeroelastic plate. *Journal of sound and vibration*, 390:141–163, 2017.

[27] Natsuki Tsushima and Weihua Su. A study on adaptive vibration control and energy conversion of highly flexible multifunctional wings. *Aerospace Science and Technology*, 79:297–309, 2018.

[28] A. Abdelkefi. Aeroelastic energy harvesting: A review. *International Journal of Engineering Science*, 100:112–135, 2016.

[29] Leonardo Sanches, Thiago AM Guimarães, and Flávio D Marques. Aeroelastic tailoring of nonlinear typical section using the method of multiple scales to predict post-flutter stable lcos. *Aerospace Science and Technology*, 90:157–168, 2019.

[30] D. Dessi, F. Mastroddi, and L. Morino. Limit-cycle stability reversal near a hopf bifurcation with aeroelastic applications. *Journal of sound and vibration*, 256(2):347–365, 2002.

[31] D. Dessi and F. Mastroddi. Limit-cycle stability reversal via singular perturbation and wing-flap flutter. *Journal of fluids and structures*, 19(6):765–783, 2004.

[32] Donald S. Woolston. An investigation of effects of certain types of structural nonhnearities on wing and control surface flutter. *Journal of the Aeronautical Sciences*, 24(1):57–63, 1957.

[33] SF Shen. An approximate analysis of nonlinear flutter problems. *Journal of the Aerospace Sciences*, 26(1):25–32, 1959.

[34] ZC Yang and LC Zhao. Analysis of limit cycle flutter of an airfoil in incompressible flow. *Journal of sound and vibration*, 123(1):1–13, 1988.

[35] DM Tang, EH Dowell, and LN Virgin. Limit cycle behavior of an airfoil with a control surface. *Journal of Fluids and Structures*, 12(7):839–858, 1998.

[36] MD Conner, DM Tang, EH Dowell, and LN Virgin. Nonlinear behavior of a typical airfoil section with control surface freeplay: a numerical and experimental study. *Journal of Fluids and structures*, 11(1):89–109, 1997.

[37] Earl Dowell, John Edwards, and Thomas Strganac. Nonlinear aeroelasticity. *Journal of aircraft*, 40(5):857–874, 2003.

[38] Deman Tang and Earl H Dowell. Flutter and limit-cycle oscillations for a wing-store model with freeplay. *Journal of Aircraft*, 43(2):487–503, 2006.

[39] Deman Tang and Earl H Dowell. Aeroelastic airfoil with free play at angle of attack with gust excitation. *AIAA journal*, 48(2):427–442, 2010.

[40] Deman Tang and Earl H Dowell. Computational/experimental aeroelastic study for a horizontal-tail model with free play. *AIAA journal*, 51(2):341–352, 2012.

[41] Hassan Elahi, Marco Eugeni, and Paolo Gaudenzi. Design and performance evaluation of a piezoelectric aeroelastic energy harvester based on the limit cycle oscillation phenomenon. *Acta Astronautica*, 157:233–240, 2019.

[42] RF Swati, LH Wen, Hassan Elahi, AA Khan, and S Shad. Extended finite element method (xfem) analysis of fiber reinforced composites for prediction of micro-crack propagation and delaminations in progressive damage: a review. *Microsystem Technologies*, 25(3):747–763, 2019.

[43] Liaosha Tang, Michael P Paı, et al. On the instability and the post-critical behaviour of two-dimensional cantilevered flexible plates in axial flow. *Journal of Sound and Vibration*, 305(1-2):97–115, 2007.